

Three Dimensional Stress Analysis of Plates Using Assumed Natural Strain Method and Sampling Surfaces Method Applied to the Four-Node Quadrilateral Plate Element

Mehdi Bohlooly¹, S.V. Plotnikova², Mohammad Ali Kouchakzadeh¹, G. M. Kulikov^{2*}

¹ Department of Aerospace Engineering, Sharif University of Technology, Azadi St., P.O. Box: 11155-8639, Tehran, Iran;

² Laboratory of Intelligent Materials and Structures, Tambov State Technical University, 106, Sovetskaya St., Tambov, 392000, Russia

*Corresponding author: +7 4752 63 04 41. E-mail: gmkulikov@mail.ru

Abstract

In the present study, the combination of the displacement-based assumed natural strain method and the sampling surfaces method is developed for the isoparametric quadrilateral four-node plate element. The distributions of displacements are considered according to a higher-order formulation which yields nonlinear transverse shear strains. The parasitic transverse shear strains are counteracted by an assumed natural strain method. Several numerical examples are presented to illustrate the benefits of the present approach for the three dimensional stress analysis of plate-type structures.

Keywords

Assumed natural strain method; sampling surface method; finite element method.

© Mehdi Bohlooly, S.V. Plotnikova, Mohammad Ali Kouchakzadeh, G.M. Kulikov, 2019

Introduction

The quadrilateral plate elements with four nodes are being increasingly used to simulate plate-type structures. The assumed natural strain (ANS) method gives the best computational efficiency of such elements for the analysis of thin-walled plates. This method avoids shear locking phenomenon by using constant-linear interpolations for assumed transverse shear strains. This condition makes pure bending deformation and there will be no parasitic transverse shear strains. Hughes and Tezduyar [1] presented displacement-based ANS method for the first time in the literature. Simo et al. [2] developed these elements for assumed stress formulations.

In order to use the quadrilateral plate elements in stress state analysis of structures, the sampling surface (SaS) method can be applied [3 – 5]. This method allows visualizing stress distribution across the thickness. Because of the complexity and time consumption of previous 3D solid elements (brick-

type) [6], the implementation of SaS method into quadrilateral plate elements is very beneficial from the performance point of view.

Besides ANS plate elements, there is a method with high computational efficiency which is named a hybrid-mixed method [7]. Kulikov and Plotnikova [8] implemented the SaS method into the hybrid-mixed method for three dimensional stress analysis of plates. The advantage of the ANS method with respect to the hybrid-mixed method is its low time consumption and equal accuracy in fine meshes. Although, the quadrilateral plate elements using ANS method have also serious drawback, which is discoverable in coarse meshes.

This paper presents the combination of the displacement-based ANS method and the SaS method to study three dimensional stress analysis of plate-type structures in different range of thickness including thin, moderately thick, and thick cases. The quadrilateral elements with four-node are applied. Multiplication of three displacements for each node by the number of

SaS is degrees of freedom per node. The accuracy of the proposed finite element formulation is studied by several examples such as bending patch test, rectangular plate under sinusoidal pressure, and circular plate under a concentrated force and supported at two points.

The Basic description of problem

A plate with arbitrary shape and uniform thickness h is shown in Fig. 1. A Cartesian coordinate system (x^1, x^2, x^3) is assumed which the origin is located on the middle surface ($x^3 = 0$) of the structure. In order to describe the structure as three dimensional solid, it is divided to finite surfaces named SaS $\Omega^I (I=1, \dots, N)$ parallel to the middle surface. The distance between these surfaces is not uniform and the position of SaS can be declared as follows:

$$Z^I = -\frac{h}{2} \cos\left(\pi \frac{2I-1}{2N}\right), \quad I=1, \dots, N. \quad (1)$$

The relation between strain coefficients $\varepsilon_{ij} (i, j=1, 2, 3)$ and displacements $u_i (i=1, 2, 3)$ is given by

$$2\varepsilon_{ij} = u_{i,j} + u_{j,i}, \quad (2)$$

here $(\cdot)_{,i}$ and $(\cdot)_{,j}$ denote derivative with respect to i and j . The strain coefficients at SaS can be calculated as

$$\begin{aligned} 2\varepsilon_{\alpha\beta}^I &= u_{\alpha,\beta}^I + u_{\beta,\alpha}^I, \\ 2\varepsilon_{\alpha 3}^I &= \kappa_{\alpha}^I + u_{3,\alpha}^I, \quad \alpha, \beta = 1, 2, \\ \varepsilon_{33}^I &= \kappa_3^I, \end{aligned} \quad (3)$$

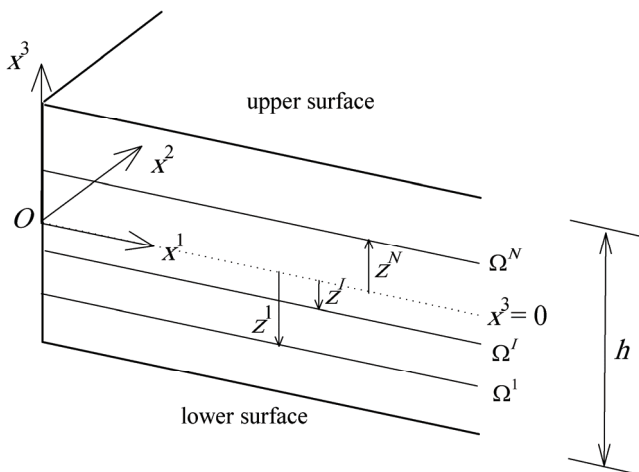


Fig. 1. A plate-type structure with a Cartesian coordinate system in the middle surface

where, I is used for numeration of SaS and $\kappa_i^I (i=1, 2, 3)$ denotes derivation of displacements with respect to coordinate x^3 .

According to a higher-order formulation, the displacements fields are assumed to be

$$u_i(x^1, x^2, x^3) = \sum_I L^I(x^3) u_i^I(x^1, x^2), \quad (4)$$

here $L^I(x^3)$ denotes the Lagrange polynomial of degree $N-1$ as follows

$$L^I = \prod_{J \neq I} \frac{x^3 - z^J}{z^I - z^J}, \quad J=1, \dots, N. \quad (5)$$

Above definition yields

$$\kappa_i^I = \sum_J M^{JI} u_{i,J}^J, \quad (6)$$

where M^{JI} denotes polynomial of degree $N-2$ as follows

$$M^{JI} = \begin{cases} \frac{1}{z^J - z^I} \prod_{K \neq I, J} \frac{z^I - z^K}{z^J - z^K}, & J \neq I; \\ -\sum_{J \neq I} M^{JI}, & J = I, \end{cases} \quad K=1, \dots, N. \quad (7)$$

The use of Eqs. (3) and (4) leads to the strain distribution

$$\varepsilon_{ij} = \sum_I L^I \varepsilon_{ij}^I. \quad (8)$$

According to Hooke's law, the stress coefficients can be derived as

$$\sigma_{ij} = \mathbf{C} \varepsilon_{ij}, \quad (9)$$

where the coefficients of matrix \mathbf{C} depend on elastic modulus and Poisson's ratio for homogenous and isotropic materials.

The Displacement-based finite element formulation

In the case of isoparametric four-node quadrilateral plate element, the position vector is approximated according to the standard C^0 interpolation

$$x^\alpha = \sum_r N_r x_r^\alpha, \quad r=1, 2, 3, 4 \quad (10)$$

and the displacement vector is defined as

$$u_i^I = \sum_r N_r u_{ir}^I, \quad (11)$$

here the bilinear shape functions of the finite elements are

$$N_r(\xi^1, \xi^2) = \frac{1}{4}(1 + n_{1r}\xi^1)(1 + n_{2r}\xi^2), \quad (12)$$

wherein $n_{11} = n_{14} = n_{21} = n_{22} = 1$ and $n_{12} = n_{13} = n_{23} = n_{24} = -1$. The parameters x_r^α and u_{ir}^I denote nodal coordinate and displacements of SaS at element nodes, respectively.

In order to avoid shear locking phenomenon and have no fictitious zero energy modes, the ANS interpolation is applied which transverse shear strains of SaS can be written as follows

$$\varepsilon_{\alpha 3}^I = \ell_{\alpha}^{\beta} \hat{\varepsilon}_{\beta 3}^I, \quad \alpha, \beta = 1, 2 \quad (13)$$

and

$$\hat{\varepsilon}_{13}^I = \frac{1}{2}(1 - \xi^2) \hat{\varepsilon}_{13}^I(B) + \frac{1}{2}(1 + \xi^2) \hat{\varepsilon}_{13}^I(D), \quad (14)$$

$$\hat{\varepsilon}_{23}^I = \frac{1}{2}(1 - \xi^1) \hat{\varepsilon}_{23}^I(A) + \frac{1}{2}(1 + \xi^1) \hat{\varepsilon}_{23}^I(C),$$

here $\hat{\varepsilon}_{\beta 3}^I$ denote the covariant components of the strain tensor of SaS. These parameters at sampling points A, B, C, and D (see Fig. 2) are obtained as

$$\begin{aligned} 2\hat{\varepsilon}_{13}^I(B) &= \frac{1}{2}(u_{34}^I - u_{33}^I) + \frac{1}{4} \sum_J M^{JJ} (x_4^\alpha - x_3^\alpha) (u_{\alpha 4}^I + u_{\alpha 3}^I), \\ 2\hat{\varepsilon}_{13}^I(D) &= \frac{1}{2}(u_{31}^I - u_{32}^I) + \frac{1}{4} \sum_J M^{JJ} (x_1^\alpha - x_2^\alpha) (u_{\alpha 1}^I + u_{\alpha 2}^I), \\ 2\hat{\varepsilon}_{23}^I(A) &= \frac{1}{2}(u_{32}^I - u_{33}^I) + \frac{1}{4} \sum_J M^{JJ} (x_2^\alpha - x_3^\alpha) (u_{\alpha 2}^I + u_{\alpha 3}^I), \\ 2\hat{\varepsilon}_{23}^I(C) &= \frac{1}{2}(u_{31}^I - u_{34}^I) + \frac{1}{4} \sum_J M^{JJ} (x_1^\alpha - x_4^\alpha) (u_{\alpha 1}^I + u_{\alpha 4}^I). \end{aligned} \quad (15)$$

To compute the derivatives of shape functions in Eq. (12) with respect to global coordinates (x^1, x^2) , the relations in Eqs. (13) – (15) are utilized as follows

$$\begin{bmatrix} \frac{\partial N_r}{\partial x^1} \\ \frac{\partial N_r}{\partial x^2} \end{bmatrix} = \mathbf{J}^{-1} \begin{bmatrix} \frac{\partial N_r}{\partial \xi^1} \\ \frac{\partial N_r}{\partial \xi^2} \end{bmatrix}, \quad (16)$$

where Jacobian matrix \mathbf{J} and its inverse \mathbf{J}^{-1} are

$$\mathbf{J} = [\ell_{\alpha}^{\beta}]_{2 \times 2}, \quad \mathbf{J}^{-1} = [\ell_{\alpha}^{\beta}]_{2 \times 2}, \quad \alpha, \beta = 1, 2, \quad (17)$$

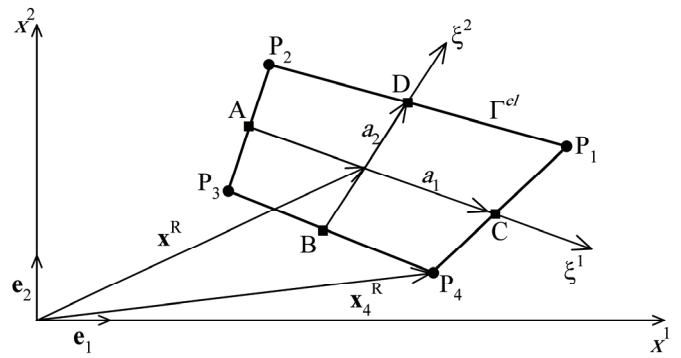


Fig. 2. Quadrilateral four node plate element

$$t_1^\alpha = \frac{1}{4}(1 + \xi^2)(x_1^\alpha - x_2^\alpha) + \frac{1}{4}(1 - \xi^2)(x_4^\alpha - x_3^\alpha),$$

$$t_2^\alpha = \frac{1}{4}(1 + \xi^1)(x_1^\alpha - x_4^\alpha) + \frac{1}{4}(1 - \xi^1)(x_2^\alpha - x_3^\alpha),$$

$$\ell_1^1 = \frac{1}{\det(\mathbf{J})} t_2^2, \quad \ell_1^2 = -\frac{1}{\det(\mathbf{J})} t_1^1,$$

$$\ell_2^1 = -\frac{1}{\det(\mathbf{J})} t_2^1, \quad \ell_2^2 = \frac{1}{\det(\mathbf{J})} t_1^2.$$

The determinant of Jacobian matrix $\det(\mathbf{J})$ can be computed as

$$\det(\mathbf{J}) = c_0 + c_1 \xi^1 + c_2 \xi^2, \quad (18)$$

wherein

$$\begin{aligned} c_0 &= \frac{1}{8} [(x_1^1 - x_3^1)(x_2^2 - x_4^2) - (x_2^1 - x_4^1)(x_1^2 - x_3^2)], \\ c_1 &= \frac{1}{8} [(x_1^1 - x_2^1)(x_3^2 - x_4^2) - (x_3^1 - x_4^1)(x_1^2 - x_2^2)], \\ c_2 &= \frac{1}{8} [(x_1^1 - x_4^1)(x_2^2 - x_3^2) - (x_2^1 - x_3^1)(x_1^2 - x_4^2)]. \end{aligned} \quad (19)$$

Substituting Eq. (4) into Eq. (3) and taking into account Eqs. (16) and (17) gives the matrix form of strain-displacement relations as follows

$$\boldsymbol{\varepsilon}^I = \mathbf{B}^I \mathbf{U}, \quad (20)$$

where

$$\mathbf{B}^I = [\varepsilon_{11}^I \quad \varepsilon_{22}^I \quad \varepsilon_{33}^I \quad 2\varepsilon_{12}^I \quad 2\varepsilon_{13}^I \quad 2\varepsilon_{23}^I]^T \quad (21)$$

and

$$\mathbf{U} = [\mathbf{U}_1^T \quad \mathbf{U}_2^T \quad \mathbf{U}_3^T \quad \mathbf{U}_4^T]^T. \quad (22)$$

Also, \mathbf{U}_r is the nodal displacement vector of the element as follows

$$\mathbf{U}_r = [u_{1r}^1 \quad u_{2r}^1 \quad u_{3r}^1 \quad u_{1r}^2 \quad u_{2r}^2 \quad u_{3r}^2 \quad \dots \quad u_{1r}^N \quad u_{2r}^N \quad u_{3r}^N]^T \quad (23)$$

and \mathbf{B}^I is strain-displacement transformation matrix of order $6 \times 12N$ which is listed in Appendix A.

By applying a variational principle and taking into account Eqs. (4) and (20), the equilibrium equations of an element can be derived as

$$\mathbf{K}\mathbf{U} = \mathbf{F}, \quad (24)$$

where \mathbf{K} is the element stiffness matrix given by

$$\mathbf{K} = \sum_I \sum_J \Lambda^{IJ} \int_{-1}^1 \int_{-1}^1 (\mathbf{B}^I)^T \mathbf{C} \mathbf{B}^J \det(\mathbf{J}) d\xi^1 d\xi^2, \quad (25)$$

where

$$\Lambda^{IJ} = \int_{-h/2}^{h/2} L^I L^J dx^3 \quad (26)$$

and \mathbf{F} is the surface traction vector with following definition

$$\mathbf{F} = [\mathbf{F}_1^T \mathbf{F}_2^T \mathbf{F}_3^T \mathbf{F}_4^T]^T,$$

$$\mathbf{F}_r = [f_{1r}^1 f_{2r}^1 f_{3r}^1 f_{1r}^2 f_{2r}^2 f_{3r}^2 \dots f_{1r}^N f_{2r}^N f_{3r}^N]^T \quad (27)$$

in which

$$f_{ir}^I = \int_{-1}^1 \int_{-1}^1 [L^I(h/2)p_i^+ - L^I(-h/2)p_i^-] N_r \det(\mathbf{J}) \xi^1 d\xi^2. \quad (28)$$

The parameters p_i^+ and p_i^- denote the distributed force in direction i of upper and lower surface, respectively. The numerical integration of Eq. (25) can be carried out by Gaussian integration scheme with 2×2 sampling points.

Numerical results

In this section, the three dimensional stress analysis for three plate problems is presented to show the accuracy of the proposed finite element formulation.

In first example, it is studied the out of plane bending behavior of quadrilateral elements using bending patch test. A rectangular plate with five elements is considered in which there are four external and four internal nodes as shown in Fig. 3. The displacements of SaS at external nodes are considered as

$$u_1^I = ez^I \left(x^1 + \frac{1}{2} x^2 \right), \quad u_2^I = ez^I \left(\frac{1}{2} x^1 + x^2 \right), \\ u_3^I = -\frac{1}{2} e \left[(x^1)^2 + x^1 x^2 + (x^2)^2 \right]. \quad (29)$$

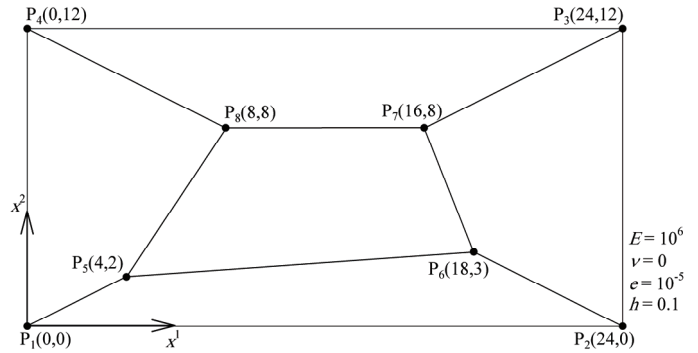


Fig. 3. A rectangular plate for bending patch test

This condition yields

$$\varepsilon_{\alpha\alpha}^I = ez^I, \quad 2\varepsilon_{12}^I = ez^I, \quad u_{i3}^I = 0. \quad (30)$$

By substitution of Eq. (29) in the boundary condition of global equilibrium equation, the displacements of internal nodes of upper surface are calculated and the results are listed in Table 1. As can be seen, this problem is solved in three different numbers of SaS as three, five, and seven. Note also that the results of exact solution [8] are listed and good agreements are achieved. Besides, the present results are slightly better than those obtained by a hybrid-mixed quadrilateral [8].

In the second example, a rectangular plate with simply supported boundary conditions is assumed. The upper surface of plate is subjected to transverse sinusoidal pressure

$$p_3^+ = p_0 \cos \frac{\pi x^1}{a} \cos \frac{\pi x^2}{b}, \quad p_3^- = 0,$$

$$-a/2 \leq x^1 \leq a/2, \quad -b/2 \leq x^2 \leq b/2, \quad (31)$$

here $p_0 = 1$ and the mechanical and geometrical properties are as follows

$$E = 10^7, \quad \nu = 0.3, \quad (32) \\ a = b = 1.$$

In order to compare the results of this problem with 3D closed form solution of Vlasov [9], the dimensionless parameters are used as follows

$$\bar{u}_1 = 100 E h^2 u_1 \left(\frac{a}{2}, 0, z \right) / (a^3 p_0),$$

$$\bar{u}_3 = 100 E h^3 u_3(0, 0, z) / (a^4 p_0),$$

$$\bar{\sigma}_{11} = 10 h^2 \sigma_{11}(0, 0, z) / (a^2 p_0),$$

$$\bar{\sigma}_{12} = 10 h^2 \sigma_{12} \left(\frac{a}{2}, \frac{a}{2}, z \right) / (a^2 p_0),$$

Table 1

Displacements of upper surface at internal nodes in the bending patch test

| Solution | Node | $u_1(h/2)$ | $u_2(h/2)$ | $-u_3(h/2)$ |
|-----------|----------------|----------------------------|----------------------------|----------------------------|
| Exact [8] | P ₅ | 2.5000000×10^{-6} | 2.0000000×10^{-6} | 1.4000000×10^{-4} |
| | P ₆ | 9.7500000×10^{-6} | 6.0000000×10^{-6} | 1.9350000×10^{-3} |
| | P ₇ | 1.0000000×10^{-5} | 8.0000000×10^{-6} | 2.2400000×10^{-3} |
| | P ₈ | 6.0000000×10^{-6} | 6.0000000×10^{-6} | 9.6000000×10^{-4} |
| $N = 3$ | P ₅ | 2.5000000×10^{-6} | 1.9999998×10^{-6} | 1.4000000×10^{-6} |
| | P ₆ | 9.7499999×10^{-6} | 5.9999999×10^{-6} | 1.9350000×10^{-3} |
| | P ₇ | 1.0000000×10^{-5} | 7.9999997×10^{-6} | 2.2399999×10^{-3} |
| | P ₈ | 5.9999996×10^{-6} | 5.9999998×10^{-6} | 9.5999997×10^{-4} |
| $N = 5$ | P ₅ | 2.4999982×10^{-6} | 2.0000000×10^{-6} | 1.3999993×10^{-4} |
| | P ₆ | 9.7500015×10^{-6} | 5.9999991×10^{-6} | 1.9349998×10^{-3} |
| | P ₇ | 1.0000002×10^{-5} | 8.0000004×10^{-6} | 2.2399997×10^{-3} |
| | P ₈ | 5.9999975×10^{-6} | 6.0000003×10^{-6} | 9.5999978×10^{-4} |
| $N = 7$ | P ₅ | 2.5000030×10^{-6} | 2.0000004×10^{-6} | 1.4000013×10^{-4} |
| | P ₆ | 9.7499972×10^{-6} | 6.0000006×10^{-6} | 1.9350001×10^{-3} |
| | P ₇ | 9.9999960×10^{-6} | 7.9999996×10^{-6} | 2.2400003×10^{-3} |
| | P ₈ | 6.0000036×10^{-6} | 5.9999986×10^{-6} | 9.6000034×10^{-4} |

Table 2

Displacements and stresses for plate ($a/h = 10$) with regular 64×64 mesh

| Solution | $\bar{u}_1(0.5)$ | $\bar{u}_3(0)$ | $\bar{\sigma}_{11}(0.5)$ | $-\bar{\sigma}_{12}(0.5)$ | $-\bar{\sigma}_{13}(0)$ | $\bar{\sigma}_{33}(0)$ |
|------------|------------------|----------------|--------------------------|---------------------------|-------------------------|------------------------|
| $N = 3$ | 4.34102 | 2.92368 | 1.99124 | 1.04863 | 1.70576 | 0.49760 |
| $N = 5$ | 4.37112 | 2.94266 | 2.00394 | 1.05590 | 2.38391 | 0.49973 |
| $N = 7$ | 4.37112 | 2.94266 | 2.00394 | 1.05590 | 2.38277 | 0.49972 |
| $N = 9$ | 4.37112 | 2.94266 | 2.00394 | 1.05590 | 2.38277 | 0.49972 |
| Vlasov [9] | 4.37064 | 2.94247 | 2.00439 | 1.05621 | 2.38337 | 0.49995 |

Table 3

Displacements and stresses for plate ($a/h = 2$) with regular 64×64 mesh

| Solution | $\bar{u}_1(0.5)$ | $\bar{u}_3(0)$ | $\bar{\sigma}_{11}(0.5)$ | $-\bar{\sigma}_{12}(0.5)$ | $-\bar{\sigma}_{13}(0)$ | $\bar{\sigma}_{33}(0)$ |
|------------|------------------|----------------|--------------------------|---------------------------|-------------------------|------------------------|
| $N = 3$ | 3.43427 | 5.61133 | 2.68269 | 0.82959 | 1.59583 | 0.44360 |
| $N = 5$ | 4.32622 | 6.04297 | 3.02669 | 1.04506 | 2.30650 | 0.47990 |
| $N = 7$ | 4.32802 | 6.04727 | 3.01309 | 1.04549 | 2.27579 | 0.47521 |
| $N = 9$ | 4.32803 | 6.04724 | 3.01277 | 1.04549 | 2.27627 | 0.47530 |
| $N = 11$ | 4.32803 | 6.04725 | 3.01276 | 1.04549 | 2.27626 | 0.47530 |
| Vlasov [9] | 4.32747 | 6.04659 | 3.01359 | 1.04578 | 2.27685 | 0.47553 |

$$\begin{aligned}\bar{\sigma}_{13} &= 10h\sigma_{13}\left(\frac{a}{2}, 0, z\right)/(ap_0), \\ \bar{\sigma}_{33} &= \sigma_{33}(0, 0, z)/p_0, \quad z = x^3/h.\end{aligned}\quad (33)$$

By modeling one quarter of the plate (due to symmetry of load and geometry) with regular 64×64 mesh of elements, the results are calculated for moderately thick ($a/h = 10$) and thick ($a/h = 2$) plates and the results are listed in Tables 2 and 3, respectively. According to these comparisons, the results are well justified with those of Vlasov [9]. The distributions of

parameters in Eq. (33) across the thickness for different plates are illustrated in Fig. 4.

In the third example, a circular plate under a concentrated load F is considered. The plate is supported at two opposite points of perimeter. Fig. 5 shows the schematic of conditions of this problem. According to symmetry, one quarter of plate is modeled by using mesh parameter of 24. The mechanical and geometrical properties are

$$\begin{aligned}E &= 10^5, \quad \nu = 0.25, \\ R &= 1.\end{aligned}\quad (34)$$

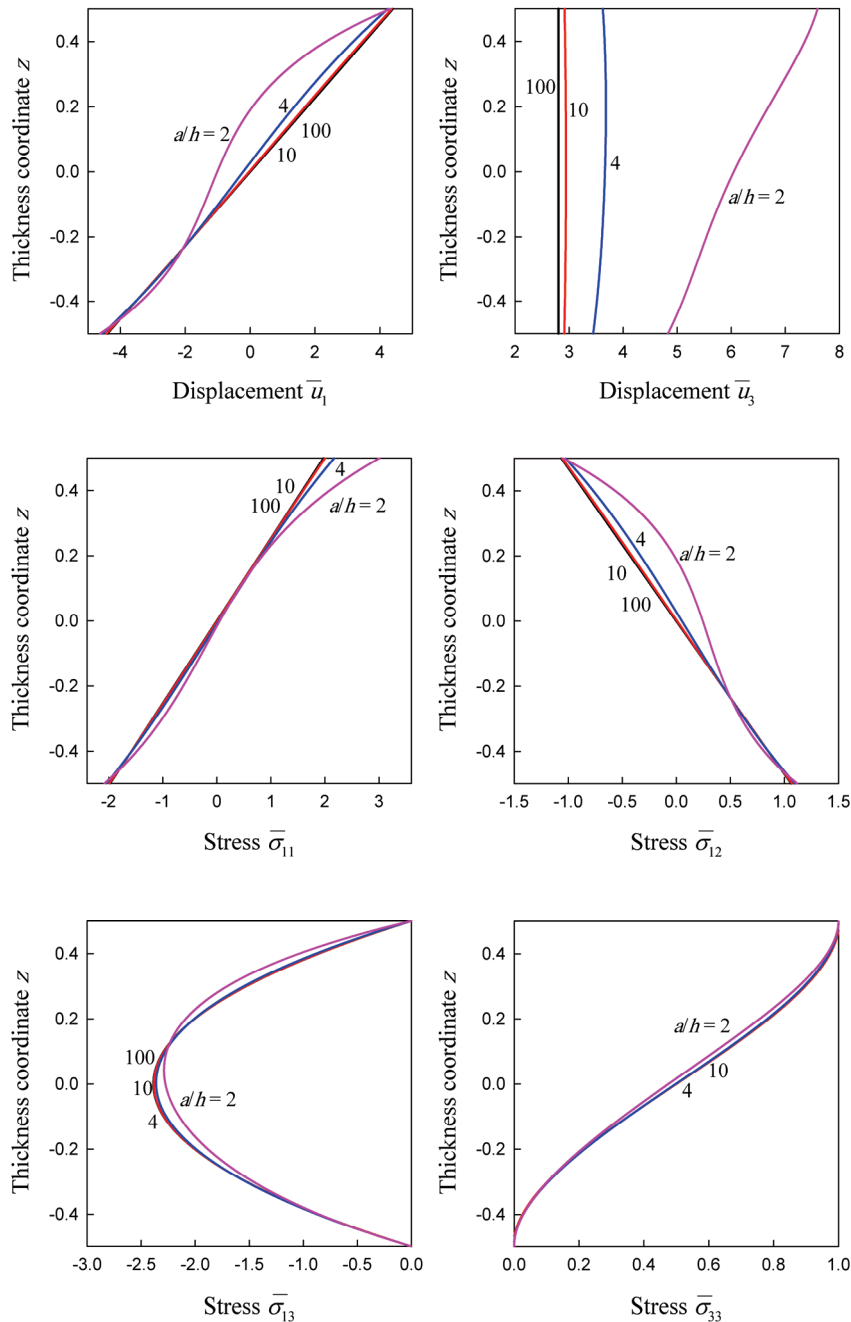


Fig. 4. Distribution of displacements and stresses for rectangular plates under sinusoidal pressure ($N = 7$)

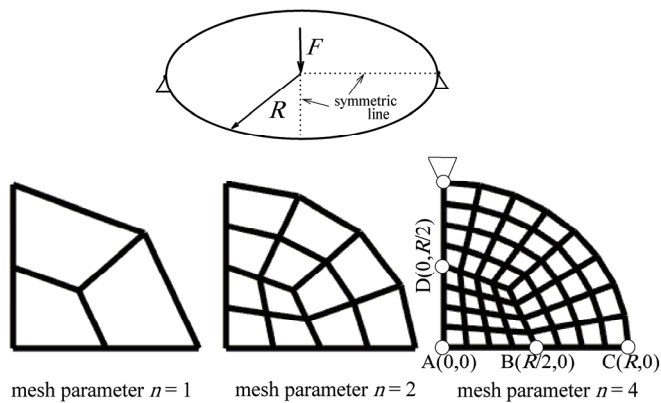


Fig. 5. Schematic of circular plate under concentrated force and supported at two points with distorted mesh by $3n^2$ elements, which $n = 1, 2, 4, 8, 16$ and 24

In order to show the results at a point $P(x^1, x^2)$, the dimensionless parameters are defined as

$$\bar{u}_1(P, z) = 10^3 Ehu_1(P, z)/(SF),$$

$$\bar{u}_2(P, z) = 10 Ehu_2(P, z)/(SF),$$

$$\bar{u}_3(P, z) = Ehu_3(P, z)/(S^2 F),$$

$$\bar{\sigma}_{11}(P, z) = 10^2 h^2 \sigma_{11}(P, z)/F,$$

$$\bar{\sigma}_{22}(P, z) = h^2 \sigma_{22}(P, z)/F,$$

$$\bar{\sigma}_{13}(P, z) = 10Sh^2 \sigma_{13}(P, z)/F,$$

$$\bar{\sigma}_{23}(P, z) = 10Sh^2 \sigma_{23}(P, z)/F,$$

$$z = x^3/h, \quad S = R/h.$$

(35)

The results of displacements and stresses at points A, B, C, and D (defined on Fig. 5) are listed in Tables 4 and 5 for thin ($S = 100$) and moderately thick ($S = 10$) circular plates. Three different numbers of SaS are used ($N = 3, 5$, and 7). The results are compared with the analytical approach via a Kirchhoff plate theory [10] and numerical results obtained by a hybrid-mixed quadrilateral [8]. It is seen that all results agree closely. The stress distributions for plates with various thicknesses are plotted in Fig. 6. As can be seen, the nonlinearity of distribution of dimensionless stress $\bar{\sigma}_{11}$ at point B is more pronounced in thicker plates.

Table 4

Displacements and stresses for circular plate ($S = 100$) with $n = 24$ (1728 elements)

| Solution | $\bar{u}_3(A, 0)$ | $\bar{u}_3(C, 0)$ | $\bar{u}_2(D, 0.5)$ | $\bar{\sigma}_{22}(D, 0.5)$ | $-\bar{\sigma}_{13}(B, 0)$ | $-\bar{\sigma}_{23}(D, 0)$ |
|-----------------|-------------------|-------------------|---------------------|-----------------------------|----------------------------|----------------------------|
| $N = 3$ | 1.31328 | 1.32892 | 6.99873 | 0.95598 | 2.59513 | 4.77445 |
| $N = 5$ | 1.31347 | 1.32915 | 6.99911 | 0.9561 | 3.66287 | 6.73437 |
| $N = 7$ | 1.31347 | 1.32915 | 6.99903 | 0.95621 | 3.66410 | 6.73533 |
| $N = 7$ [8] | 1.3135 | 1.3292 | 6.9988 | 0.95389 | 3.5505 | 6.6357 |
| Timoshenko [10] | 1.31 | 1.33 | | | — | |

Table 5

Displacements and stresses for circular plate ($S = 10$) with $n = 24$ (1728 elements)

| Solution | $\bar{u}_3(A, 0)$ | $\bar{u}_3(C, 0)$ | $\bar{u}_2(D, 0.5)$ | $\bar{\sigma}_{22}(D, 0.5)$ | $-\bar{\sigma}_{13}(B, 0)$ | $-\bar{\sigma}_{23}(D, 0)$ |
|-------------|-------------------|-------------------|---------------------|-----------------------------|----------------------------|----------------------------|
| $N = 3$ | 1.36056 | 1.37558 | 7.03997 | 0.97389 | 2.63468 | 4.65461 |
| $N = 5$ | 1.37065 | 1.38149 | 7.05443 | 0.97569 | 3.72610 | 6.55463 |
| $N = 7$ | 1.37126 | 1.38163 | 7.05447 | 0.97572 | 3.72627 | 6.55494 |
| $N = 7$ [8] | 1.3710 | 1.3817 | 7.0488 | 0.97536 | 3.6620 | 6.5344 |

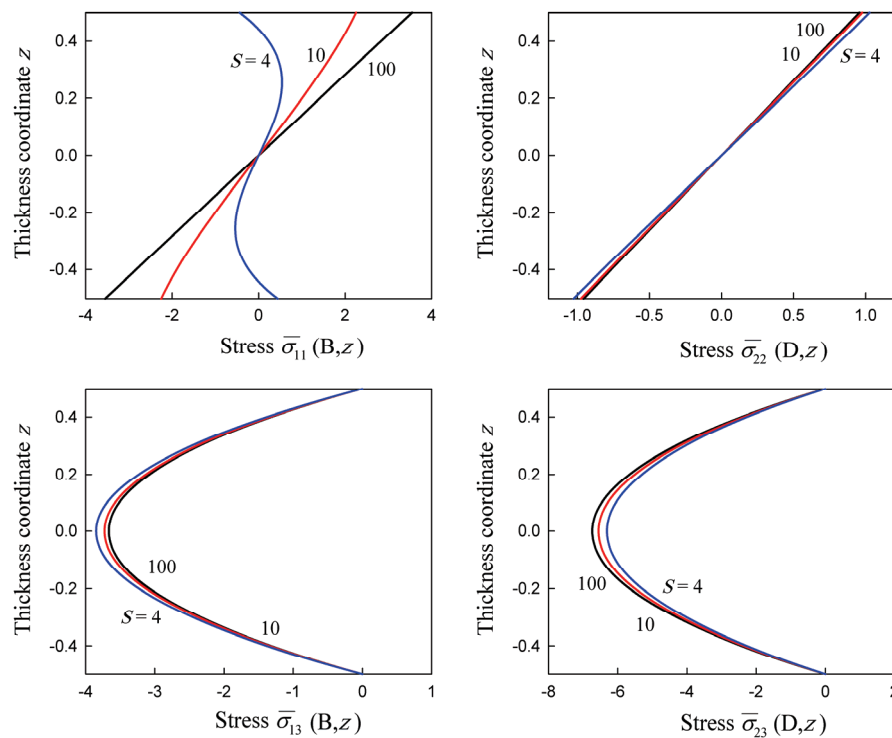


Fig. 6. Distribution of stresses for circular plates under concentrated force with $n = 24$ (1728 elements)

Conclusion

The quadrilateral four-node element using the displacement-based ANS method and the SaS method is presented in this paper. The application of the SaS method gives an opportunity to derive stress distribution across the thickness. These distributions are more useful for thicker structures which transverse shear strains are not negligible. Some examples including rectangular and circular plates under different loads are presented to highlight the benefits of current three dimensional analysis of structures.

References

1. Hughes T.J., Tezduyar T. Finite elements based upon Mindlin plate theory with particular reference to the four-node bilinear isoparametric element. *Journal of Applied Mechanics*, 1981, vol. 48 (3), pp. 587-96.
2. Simo J., Rifai M., Fox D. On a stress resultant geometrically exact shell model. Part IV: Variable thickness shells with through-the-thickness stretching. *Computer Methods in Applied Mechanics and Engineering*, 1990, vol. 81 (1), pp. 91-126.
3. Kulikov G.M., Plotnikova S.V. On the use of sampling surfaces method for solution of 3D elasticity problems for thick shells. *ZAMM – Journal of Applied Mathematics and Mechanics / Zeitschrift für Angewandte Mathematik und Mechanik*, 2012, vol. 92 (11-12), pp. 910-20.
4. Kulikov G.M., Plotnikova S.V. Exact 3D stress analysis of laminated composite plates by sampling surfaces method. *Composite Structures*, 2012, vol. 94 (12), pp. 3654-63.
5. Kulikov G.M., Plotnikova S.V. Advanced formulation for laminated composite shells: 3D stress analysis and rigid-body motions. *Composite Structures*, 2013, vol. 95, pp. 236-46.
6. Cheung Y, Wanji C. Isoparametric hybrid hexahedral elements for three dimensional stress analysis. *International Journal for Numerical Methods in Engineering*, 1988, vol. 26 (3), pp. 677-93.
7. Pian T.H. Derivation of element stiffness matrices by assumed stress distributions. *AIAA Journal*, 1964, vol. 2 (7), pp. 1333-6.
8. Kulikov G.M., Plotnikova S.V. A hybrid-mixed four-node quadrilateral plate element based on sampling surfaces method for 3D stress analysis. *International Journal for Numerical Methods in Engineering*, 2016, vol. 108 (1), pp. 26-54.
9. Vlasov B. On one case of bending of rectangular thick plates. *Vestnik Moskovskogo Universiteta. Seria Matematiki, Mekhaniki, Astronomii, Fiziki, Khimii*, 1957, vol. 2, pp. 25-34 (Russian).
10. Timoshenko S.P., Woinowsky-Krieger S. Theory of plates and shells: McGraw-Hill; 1959.

Appendix A

Here, the non-vanishing elements of the matrix $\mathbf{B}' = [\mathbf{B}'_1 \ \mathbf{B}'_2 \ \mathbf{B}'_3 \ \mathbf{B}'_4]$ are presented, where \mathbf{B}'_r denotes the nodal strain-displacement matrix related to SaS of order $6 \times 3N$ as follows:

$$(\mathbf{B}'_r)_{1, 3N(r-1)+3I-2} = \frac{\partial N_r}{\partial x^1}, \quad (\mathbf{B}'_r)_{2, 3N(r-1)+3I-1} = \frac{\partial N_r}{\partial x^2},$$

$$(\mathbf{B}'_r)_{3, 3N(r-1)+3J} = M^{JJ} N_r, \quad (\mathbf{B}'_r)_{4, 3N(r-1)+3I-2} = \frac{\partial N_r}{\partial x^2},$$

$$(\mathbf{B}'_r)_{4, 3N(r-1)+3I-1} = \frac{\partial N_r}{\partial x^1},$$

$$(\mathbf{B}'_1)_{5, 3J-2} = \frac{1}{4} M^{JJ} [l_1^1 t_1^1(D)(1+\xi^2) + l_1^2 t_2^1(C)(1+\xi^1)],$$

$$(\mathbf{B}'_1)_{5, 3J-1} = \frac{1}{4} M^{JJ} [l_1^1 t_1^2(D)(1+\xi^2) + l_1^2 t_2^2(C)(1+\xi^1)],$$

$$(\mathbf{B}'_1)_{5, 3I} = \frac{1}{4} [l_1^1(1+\xi^2) + l_1^2(1+\xi^1)],$$

$$(\mathbf{B}'_2)_{5, 3N+3J-2} = \frac{1}{4} M^{JJ} [l_1^1 t_1^1(D)(1+\xi^2) + l_1^2 t_2^1(A)(1-\xi^1)],$$

$$(\mathbf{B}'_2)_{5, 3N+3J-1} = \frac{1}{4} M^{JJ} [l_1^1 t_1^2(D)(1+\xi^2) + l_1^2 t_2^2(A)(1-\xi^1)],$$

$$(\mathbf{B}'_2)_{5, 3N+3I} = \frac{1}{4} [-l_1^1(1+\xi^2) + l_1^2(1-\xi^1)],$$

$$(\mathbf{B}'_3)_{5, 6N+3J-2} = \frac{1}{4} M^{JJ} [l_1^1 t_1^1(B)(1-\xi^2) + l_1^2 t_2^1(A)(1-\xi^1)],$$

$$(\mathbf{B}'_3)_{5, 6N+3J-1} = \frac{1}{4} M^{JJ} [l_1^1 t_1^2(B)(1-\xi^2) + l_1^2 t_2^2(A)(1-\xi^1)],$$

$$(\mathbf{B}'_3)_{5, 6N+3I} = \frac{1}{4} [-l_1^1(1-\xi^2) - l_1^2(1-\xi^1)],$$

$$(\mathbf{B}'_4)_{5, 9N+3J-2} = \frac{1}{4} M^{JJ} [l_1^1 t_1^1(B)(1-\xi^2) + l_1^2 t_2^1(C)(1+\xi^1)],$$

$$(\mathbf{B}'_4)_{5, 9N+3J-1} = \frac{1}{4} M^{JJ} [l_1^1 t_1^2(B)(1-\xi^2) + l_1^2 t_2^2(C)(1+\xi^1)],$$

$$(\mathbf{B}'_4)_{5, 9N+3I} = \frac{1}{4} [l_1^1(1-\xi^2) - l_1^2(1+\xi^1)],$$

$$(\mathbf{B}'_1)_{6, 3J-2} = \frac{1}{4} M^{JJ} [l_2^1 t_1^1(D)(1+\xi^2) + l_2^2 t_2^1(C)(1+\xi^1)],$$

$$(\mathbf{B}'_1)_{6, 3J-1} = \frac{1}{4} M^{JJ} [l_2^1 t_1^2(D)(1+\xi^2) + l_2^2 t_2^2(C)(1+\xi^1)],$$

$$(\mathbf{B}'_1)_{6, 3I} = \frac{1}{4} [l_2^1(1+\xi^2) + l_2^2(1+\xi^1)],$$

$$(\mathbf{B}'_2)_{6, 3N+3J-2} = \frac{1}{4} M^{JJ} [l_2^1 t_1^1(D)(1+\xi^2) + l_2^2 t_2^1(A)(1-\xi^1)],$$

$$(\mathbf{B}'_2)_{6, 3N+3J-1} = \frac{1}{4} M^{JJ} [l_2^1 t_1^2(D)(1+\xi^2) + l_2^2 t_2^2(A)(1-\xi^1)],$$

$$(\mathbf{B}'_2)_{6, 3N+3I} = \frac{1}{4} [-l_2^1(1+\xi^2) + l_2^2(1-\xi^1)],$$

$$(\mathbf{B}'_3)_{6, 6N+3J-2} = \frac{1}{4} M^{JJ} [l_2^1 t_1^1(B)(1-\xi^2) + l_2^2 t_2^1(A)(1-\xi^1)],$$

$$(\mathbf{B}'_3)_{6, 6N+3J-1} = \frac{1}{4} M^{JJ} [l_2^1 t_1^2(B)(1-\xi^2) + l_2^2 t_2^2(A)(1-\xi^1)],$$

$$(\mathbf{B}'_3)_{6, 6N+3I} = \frac{1}{4} [-l_2^1(1-\xi^2) - l_2^2(1-\xi^1)],$$

$$(\mathbf{B}'_4)_{6, 9N+3J-2} = \frac{1}{4} M^{JJ} [l_2^1 t_1^1(B)(1-\xi^2) + l_2^2 t_2^1(C)(1+\xi^1)],$$

$$(\mathbf{B}'_4)_{6, 9N+3J-1} = \frac{1}{4} M^{JJ} [l_2^1 t_1^2(B)(1-\xi^2) + l_2^2 t_2^2(C)(1+\xi^1)],$$

$$(\mathbf{B}'_4)_{6, 9N+3I} = \frac{1}{4} [l_2^1(1-\xi^2) - l_2^2(1+\xi^1)],$$

and

$$t_1^\alpha(B) = \frac{1}{2}(x_4^\alpha - x_3^\alpha), \quad t_1^\alpha(D) = \frac{1}{2}(x_1^\alpha - x_2^\alpha),$$

$$t_2^\alpha(A) = \frac{1}{2}(x_4^\alpha - x_3^\alpha), \quad t_2^\alpha(C) = \frac{1}{2}(x_1^\alpha - x_4^\alpha).$$

The other components of the matrix \mathbf{B}'_r are equal to zero.